Precision medicine integrating whole-genome sequencing, comprehensive metabolomics, and advanced imaging

Ying-Chen Claire Hou[a], Hung-Chun Yu[a], Rick Martin[a], Elizabeth T. Cirulli[a], Natalie M. Schenker-Ahmed[a,b], Michael Hicks[a], Isaac V. Cohen[a,c], Thomas J. Jönsson[d], Robyn Heister[a], Lori Napier[a], Christine Leon Swisher[a], Saints Dominguez[a], Haibao Tang[a], Weizhong Li[e], Bradley A. Perkins[a], Jaime Barea[a], Christina Rybak[a], Emily Smith[a], Keegan Duchicela[a], Michael Doney[a], Pamila Brar[a,e], Nathaniel Hernandez[a], Ewen F. Kirkness[e], Andrew M. Kahn[a,f], J. Craig Venter[a,e], David S. Karow[a,b], and C. Thomas Caskey[a,g,1]

[a]Human Longevity, Inc., San Diego, CA 92121; [b]Department of Radiology, University of California San Diego School of Medicine, San Diego, CA 92093; [c]Skaggs School of Pharmacy and Pharmaceutical Sciences, University of California San Diego, San Diego, CA 92093; [d]Metabolon, Inc., Morrisville, NC 27713; [e]J. Craig Venter Institute, La Jolla, CA 92037; [f]Division of Cardiovascular Medicine, University of California San Diego School of Medicine, San Diego, CA 92037; and [g]Molecular and Human Genetics, Baylor College of Medicine, Houston, TX 77030

Edited by Stephen T. Warren, Emory University School of Medicine, Atlanta, GA, and approved December 24, 2019 (received for review May 30, 2019)

Genome sequencing has established clinical utility for rare disease diagnosis. While increasing numbers of individuals have undergone elective genome sequencing, a comprehensive study surveying genome-wide disease-associated genes in adults with deep phenotyping has not been reported. Here we report the results of a 3-y precision medicine study with a goal to integrate whole-genome sequencing with deep phenotyping. A cohort of 1,190 adult participants (402 female [33.8%]; mean age, 54 y [range 20 to 89+]; 70.6% European) had whole-genome sequencing, and were deeply phenotyped using metabolomics, advanced imaging, and clinical laboratory tests in addition to family/medical history. Of 1,190 adults, 206 (17.3%) had at least 1 genetic variant with pathogenic (P) or likely pathogenic (LP) assessment that suggests a predisposition of genetic risk. A multidisciplinary clinical team reviewed all reportable findings for the assessment of genotype and phenotype associations, and 137 (11.5%) had genotype and phenotype associations. A high percentage of genotype and phenotype associations (>75%) was observed for dyslipidemia ($n = 24$), cardiomyopathy, arrhythmia, and other cardiac diseases ($n = 42$), and diabetes and endocrine diseases ($n = 17$). A lack of genotype and phenotype associations, a potential burden for patient care, was observed in 69 (5.8%) individuals with P/LP variants. Genomics and metabolomics associations identified 61 (5.1%) heterozygotes with phenotype manifestations affecting serum metabolite levels in amino acid, lipid and cofactor, and vitamin pathways. Our descriptive analysis provides results on the integration of whole-genome sequencing and deep phenotyping for clinical assessments in adults.

genomics | advanced imaging | precision medicine | deep phenotyping | metabolomics

The completion of the Human Genome Project is an opportunity to use an individual's genetic variability for individualized diagnosis, disease prediction, and care (1, 2). Whole-exome or -genome sequencing (WES/WGS) has been employed as a diagnostic tool in medicine, and molecular diagnosis rates have been achieved in 17.5 to 32% of adult patients with various undiagnosed diseases (3–5). Predisposition genome sequencing in healthy adults has demonstrated medical, behavioral, and economic outcomes of using genomic sequencing information in healthy adults (6–11). From the perspective of population-based studies, the implementation of WES in the health system with longitudinal electronic health records (EHRs) has enabled the assessment of genetic risk in a wide range of diseases. The initial results from the DiscovEHR study have shown that 3.5% of individuals had clinically actionable genetic variants surveying 76 genes, and ∼2.3% of individuals who carry pathogenic variants had associated phenotypes observed in their medical records (12). The recent results from the UK Biobank, a prospective study of 49,960 individuals with extensive phenotypic data, showed that by surveying the American College of Medical Genetics and Genomics (ACMG) 59 genes, 2% of the population has a pathogenic or likely pathogenic variant requiring medical care surveillance (13). The value of genome sequencing in medicine is emerging; however, a comprehensive study surveying genome-wide disease-associated genes in adults with deep phenotyping concurrently has not been reported. Insights from integrating genomic and phenotypic information can provide useful insights as we develop the blueprint for precision medicine practice.

Significance

To understand the value and clinical impact of surveying genome-wide disease-causing genes and variants, we used a prospective cohort study design that enrolled volunteers who agreed to have their whole genome sequenced and to participate in deep phenotyping using clinical laboratory tests, metabolomics technologies, and advanced noninvasive imaging. The genomic results are integrated with the phenotype results. Approximately 1 in 6 adult individuals (17.3%) had genetic findings and, when integrated with deep phenotyping data, including family/medical histories with genetic findings, 1 in 9 (11.5%) had genotype and phenotype associations. Genomics and metabolomics association analysis revealed 5.1% of heterozygotes with phenotype manifestations affecting serum metabolite levels. We report observations from our study in which health outcomes and benefits were not measured.

Author contributions: J.C.V. conceived the study; C.T.C. led the analyses; Y.-C.C.H., H.-C.Y., R.M., and C.T.C. performed genomic analyses and genetic-phenotypic integration analysis; N.M.S.-A., C.L.S., S.D., N.H., A.M.K., and D.S.K. evaluated clinical imaging; Y.-C.C.H., H.-C.Y., R.M., R.H., J.B., C.R., E.S., K.D., M.D., P.B., and C.T.C. contributed to clinical genetics evaluation. Y.-C.C.H., H.-C.Y., E.T.C., I.V.C., and T.J.J. performed metabolomics analysis; L.N. contributed to data collection; M.H., H.T., W.L., and E.F.K. contributed to bioinformatics; R.M. R.H., J.B., C.R., E.S., K.D., M.D., P.B., A.M.K., D.S.K., and C.T.C. contributed to clinical support; B.A.P, **D.S.K.,** and C.T.C supervised research; and Y.-C.C.H., H.-C.Y., N.M.S.-A., and C.T.C. wrote the paper.

Competing interest statement: Y.-C.C.H., H.-C.Y., N.M.S.-A., R.H., L.N., S.D., K.D., P.B., N.H., A.M.K., J.C.V., D.S.K., and C.T.C. are employees of Human Longevity, Inc.

This article is a PNAS Direct Submission.

[1]To whom correspondence may be addressed. Email: tcaskey@bcm.edu.

This article contains supporting information online at https://www.pnas.org/lookup/suppl/doi:10.1073/pnas.1909378117/-/DCSupplemental.

First published January 24, 2020.

Understanding the functional consequence of genomic variation has been challenging, and numerous approaches have been employed. Molecular technologies, including metabolomics (metabolites), transcriptomics (RNA), proteomics (proteins), and epigenomics, have been employed to interpret the functional consequence of genomic variations (14–17). In particular, the diagnosis of monogenic conditions in pediatric cases has been transformed by methods that allow interrogation of biochemical and genetic data for discoveries of new associations between metabolic disorders and genes (18–20). From large-scale genome studies, the use of extensive phenotypic data in EHRs and identification of loss-of-function (LoF) variants from exome-sequencing data have improved our understanding of previously undiscovered biological functions for genes and the development of therapeutic targets (12, 21, 22).

To understand the value and impact of surveying genome-wide disease-causing genes and variants integrated with deep phenotyping, we used a prospective cohort design enrolling volunteers under a research protocol. The deep phenotyping included family history, past and current personal medical history, clinical laboratory tests, advanced noninvasive imaging, and metabolomics technologies. The study objectives were fourfold. First, we evaluated genotype and phenotype associations in adult participants in various disease areas, including cancer, cardiomyopathy, arrhythmia, and other cardiac diseases, dyslipidemia, diabetes and endocrine, chronic liver, hematology, inborn errors of metabolism, and other disorders. Second, we showed cases where the lack of genotype and phenotype associations may result in possible ambiguous results for patient care from surveying genome-wide disease-causing variants in adults with elective genome sequencing. Third, we interrogated observed cases for autosomal recessive carriers with a phenotype manifestation in imaging or metabolome. Finally, we pursued research activities using WGS with deep phenotype data. We investigated gene associations with serum metabolite changes and cholesterol homeostasis.

Results

Phenotype Test Findings. The cohort was composed of 1,190 self-referred volunteers with a median age of 54 y (range 20 to 89+ y, 33.8% female, 70.6% European). The demographic information of the cohort is shown in Table 1, and previously identified conditions (%) included cancer (11.0%), coronary heart disease (4.8%), diabetes (3.8%), chronic liver diseases (5.1%), and neurological disorders (10.2%). Our cohort had no enrichment of frequent adult chronic diseases compared with National Health and Nutrition Examination Survey (NHANES) adults, a US population-based sample. This study is an expansion of our pilot study of 209 study participants (19). We added noninvasive computed tomography (CT) of the heart to measure the amount of calcified plaque in the coronary arteries as a means of evaluating risk of coronary artery disease. The dual-energy X-ray absorptiometry test was removed. Detailed protocols used for whole-body MRI are listed in *SI Appendix*, Table S1. The criteria for cardiovascular reportable findings are listed in *SI Appendix*, Table S2 and reference ranges for clinical tests are provided in *SI Appendix*, Table S3. Each test was evaluated and assessed by board-certified physicians. Reportable findings of MRI, echocardiography (ECHO), electrocardiography (ECG), continuous cardiac monitoring (CCM), and CT are listed in *SI Appendix*, Tables S4–S7.

A heatmap representation of reportable findings from quantitative phenotype measurements of each study participant is provided in Fig. 1*B* in chronological order. Except for the CT test that was added after the pilot study, study participants had choices to omit certain tests based on medical decisions or personal preference; omissions are highlighted in gray in Fig. 1*B*. Phenotype testing revealed 407 (34.2%) participants had insulin resistance and/or impaired glucose tolerance; 343 (29.2%) participants had elevated liver fat (>4%); 193 (16.2%) participants had cardiac structure or function abnormalities; 136 (11.4%) participants had coronary heart disease risk (Agatston score > 100, relative risk [RR] 4.3) (23); 104 (9.3%) participants had elevated liver

Table 1. Study characteristics

Characteristics	This study	NHANES
Age, y		
Median (range)	54 (20 to 89+)	
Sex, %		
Male	66.2	
Female	33.8	
Measured BMI, median (25 to 75%)	25.3 (23.0 to 28.0)	
Measured systolic blood pressure, median (25 to 75%)	124 (115 to 136)	
Measured LDL, median (25 to 75%)	114 (92 to 137)	
Diseases		
Neoplasms, % (ever told you had cancer or malignancy)	11.0	9.5
Cardiovascular, % (ever told you had coronary heart disease)	4.8	4.0
Chronic respiratory diseases, % (ever told you had COPD)	2.7	3.3
Diabetes, % (ever told you have diabetes)	3.8	7.5
Chronic liver diseases, % (ever told you had liver diseases)	5.1	4.1
Neurological disorders, % (blood relatives have Alzheimer's disease or dementia)	10.2	13.3
Risk factors		
Alcohol use, %	49.5	
Tobacco smoking, %	19.6	
High cholesterol, %		
Ever told you had high cholesterol	31.5	
Taking prescription for high cholesterol	18.2	
High blood pressure, %		
Ever told you had high blood pressure	19.0	
Taking prescription for hypertension	14.6	

The NHANES information is at https://www.cdc.gov/nchs/nhanes/. COPD, chronic obstructive pulmonary disease.

iron (R2* > 80); 73 (6.1%) participants had arrhythmia; 57 (4.8%) participants had cardiac conduction disorders; and 23 (2.0%) showed low hippocampal occupancy score (≤0.65). We identified 20 (1.7%) individuals with early-stage neoplasia, prostate adenocarcinoma, renal cell carcinoma, lymphoma, transitional cell carcinoma, papillary thyroid cancer, pancreatic cancer, neurofibromatosis, and mediastinal thymoma. Among these, 12 cases were confirmed with a biopsy, 4 cases were confirmed with CT, 3 cases were surgically removed, and 1 case was confirmed by the genetic finding (*SI Appendix*, Table S4). The clinical laboratory tests that assessed cancer and liver, kidney, hematology, endocrine, immunology, and lipid functions are shown in *SI Appendix*, Fig. S1.

We also calculated the age distribution of participants with reportable findings compared with those without reportable findings in each of the tests. The age distribution of each test is provided in *SI Appendix*, Fig. S2. The median age of participants with genetic findings and extreme metabolite findings was similar compared with participants without findings ($P > 0.05$). The median ages (interquartile range) of participants with reportable findings in ECHO, CT, and CCM tests were ECHO: 62 (55 to 70); CT: 65 (57 to 70); and CCM: 64 (57 to 70). The median ages of participants with reportable findings in MRI-body, MRI-brain, and MRI-cancer diagnosed in this study were MRI-body: 55 (47 to 64); MRI-brain: 70 (52 to 76); and MRI-cancer: 64.5 (56 to 71).

Identification of Sequence Variants with Pathogenicity. To understand the value and impact of surveying genome-wide disease-causing genes and variants, we used a 2-step process described in *Materials and Methods* to filter and manually interpret each disease-causing variant per participant. We followed the American College of Medical Genetics and Genomics/Association for Molecular Pathology guidelines for the interpretation of sequence variants. Our 2-step process evaluates variants in 30,281 unique genes present in ClinVar, Human Gene Mutation Database (HGMD), and Online Mendelian Inheritance in Man (OMIM). In our cohort, 206 (17.3%) participants had at least one medically significant genetic finding (MSF) with a clinical significance of pathogenic (P), likely pathogenic (LP), or variant of unknown significance-reportable (VUS-R). The medically significant findings included heterozygotes in autosomal dominant or X-linked recessive conditions or homozygotes or compound heterozygotes in autosomal recessive conditions. The most commonly affected genes (number of cases) for autosomal dominant conditions were *CHEK2* (17), *MYBPC3* (8), *BRCA2* (7), *ATM* (6), *HOXB13* (6), and *LDLR* (6). For autosomal recessive conditions, the most commonly affected genes were *HFE* (15), *BTD* (5), and *GJB2* (2). For X-linked recessive conditions, we identified 2 cases in the *G6PD* gene. In the ACMG 59 genes, 29 individuals (2.4%) had P or LP variants identified. Frequently observed risk alleles, including *F2* c.*97G>A, *F5* Leiden c.1601G>A, and *ALDH2* c.1510G>A variants, were observed in 83 individuals (7%) of this cohort.

The assertion of pathogenicity of a genomic sequence variant is not equivalent to the clinical diagnosis of genetic disorders. Our multidisciplinary team integrated the genomic findings and evaluated whether a participant's clinical characteristics and family/personal history provided sufficient evidence to support clinical diagnosis of genetic disorders. Clinical characteristics listed in OMIM clinical synopses (24) or publications such as GeneReviews or primary studies were employed to evaluate genotype–phenotype associations. For example, for a participant with a pathogenic variant observed in the *LDLR* gene, the team would review his/her results in clinical laboratory tests and metabolome for lipid profiles, and CT scan for calcified plaque along with family/personal history. For a participant with a pathogenic variant observed in the *HNF1B* gene, the team would review his/her results in clinical laboratory tests and metabolome for profiles that are indicators of impaired glucose tolerance or impaired insulin sensitivity, and MRI test for renal cysts. Genotype and phenotype associations were identified in 137 (11.5%) participants among 206 participants with at least 1 MSF (Fig. 2). Dyslipidemia, cardiomyopathy and arrhythmia, and diabetes and endocrine diseases had associations between genotype and phenotype higher than 75% (24/24 [100%], 36/42 [85.7%], and 13/17 [76.5%], respectively). The details of genes, variants, and associated phenotypes are provided in Dataset S1 (MSF and Phenotype Associations) for 206 participants with MSFs.

Integration of advanced imaging and genomic sequencing led to the clinical diagnosis of genetic disorders which were not established previously (Fig. 3). In individuals with the *HNF1B*, *PKD1*, *PCSK9*, *MYH7*, *NF1*, and *CFTR* variants (Fig. 3 *A*–*G*), whole-body (WB)-MRI, CT, and genetic findings of variants with pathogenicity provided evidence to support the diagnosis of inherited genetic diseases. A diagnosis of renal cysts and diabetes syndrome was made in the participant with a likely pathogenic variant in the *HNF1B* gene without family/personal medical history. The imaging findings found multiple subcentimeter cysts in kidney bilaterally (Fig. 3*A*). The metabolome-based clinical tests showed impaired glucose tolerance and insulin sensitivity. The detection of a pathogenic variant in the *NF1* gene (de novo) was seen in an individual with optic glioma, white matter lesions, stenosis in the middle cerebral artery, and Moyamoya syndrome (Fig. 3 *E* and *F*). A diagnosis of cystic fibrosis was made in a mid-50s male participant. He had a history of digestive symptoms and chronic sinus infections and the imaging findings found tree-in-bud nodularity at the right mid and upper lung zone and mild bronchial wall thickening (Fig. 3*G*). Two variants, c.3846G>A (p.Trp1282*) and c.3454G>C (p.Asp1152His), were identified in the *CFTR* gene. Results from genetics and clinical presentations were consistent with atypical cystic fibrosis. We selected 12 cases to illustrate the data integration of our tests for clinical assessments (Fig. 3*I*). The integration of genomic data assisted new clinical diagnosis of genetic diseases.

Prevalence of P/LP Variants without Disease Symptoms or Family History. The identification of a genomic variant with assertion of pathogenicity does not indicate a clinical diagnosis of associated genetic disorders. Integrating genomic data with deep phenotyping presented an opportunity to further understand the lack of genotype and phenotype associations which may result in uncertainty in patient care. We report the prevalence of the P/LP variants per disease category (Table 2). For example, after carefully examining data from family history, past medical history, and advanced imaging tests, 30 out of 69 participants with P/LP variants associated with cancer predisposition did not have corresponding family history and phenotypes at the time of evaluation. The most commonly detected cancer variants (number of cases) were *HOXB13* c.251G>A (6), *CHEK2* c.470T>C (5), *CHEK2* c.1283C>T (2), and *FH* c.1431_1433dupAAA (2). Three homozygotes and 2 compound heterozygotes with P/LP variants in the *BTD* gene did not have expected elevated beta-hydroxyisovalerate and lactate phenotypes. Four compound heterozygotes with P/LP variants in the *HFE* gene also did not have expected elevated liver iron (R2*), ferritin, and iron phenotypes.

Autosomal Recessive Genetic Variants with Phenotype Manifestations. Using the genome-wide approach, 1,027 (86.3%) individuals had at least 1 autosomal recessive variant in 680 genes (Dataset S1, Autosomal Recessive Conditions and Autosomal Recessive Variants). The most commonly detected genes (number of cases) were *SERPINA1* (99), *FLG* (95), *BTD* (84), *HFE* (84), and *GJB2* (71) (*SI Appendix*, Table S8). Eighteen genes (>1% observed frequency) not commonly found in gene panels for prenatal carrier

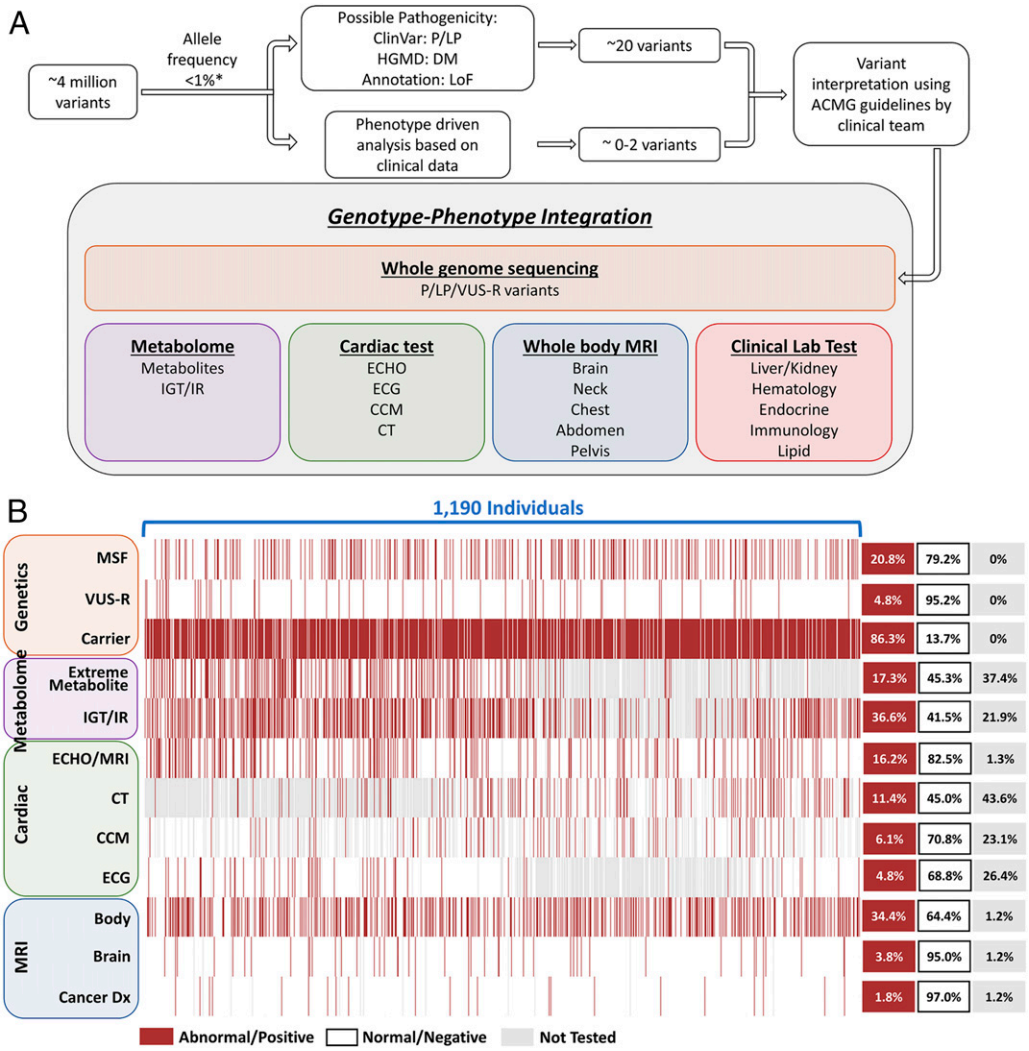

Fig. 1. Summary of all tests and results. (*A*) Diagram of study process. Organs screened by whole-body MRI: brain: neck, orbits, paranasal sinuses, skull base, nasopharynx, suprahyoid/infrahyoid neck, thyroid, thoracic inlet, lymph nodes, vascular structures, and marrow; chest: lungs and large airways, pleura, heart, mediastinum and hila, chest wall, vessels, and marrow; abdomen: liver, bile ducts, gallbladder, pancreas, spleen, adrenals, kidneys, bowel, mesenteric lymph nodes, peritoneum, retroperitoneum, abdominal wall, and marrow; pelvis: reproductive organs, bladder, bowel, peritoneum, abdominal wall, and marrow. The asterisk indicates a list of 13 variants with allele frequency higher than 1% provided in *SI Appendix*. (*B*) Heatmap of all test results listed chronologically. Cancer Dx, cancer cases diagnosed in this study; CT, computed tomography coronary artery calcium scoring; DM, damaging variant defined by HGMD; ECHO/MRI, union of the dataset of echocardiography and cardiac MRI; IGT, impaired glucose tolerance test; IR, insulin resistance test; LoF, loss-of-function variant.

screening were identified (*SI Appendix*, Table S8). We observed that carriers of autosomal recessive conditions had phenotype manifestations. Findings of *PKDH1* (Fig. 3*H*) (autosomal recessive polycystic kidney disease), *ALPL* (hypophosphatasia), and *LMBRD1* (methylmalonic aciduria and homocystinuria) are shown in Table 3. For hemochromatosis, 18% (12/68) of heterozygotes for the *HFE* p.Cys282Tyr variant had high R2*, a marker of liver iron content, compared with only 8% (87/1,034) of individuals with normal genotype ($P = 0.0156$, Fisher exact test), suggesting iron regulation is compromised. One participant with a low 10-y risk Framingham score (<5%) (25) had an Agatston score of 2,963 (RR 10.8) at the 99th percentile for people of the same age, sex, and race/ethnicity per the Multi-Ethnic Study of Atherosclerosis (25, 26). In this participant's WGS, we identified an LoF variant, c.63dupA (p.Leu22fs), in the *LMBRD1* gene in the heterozygous state with phenotypic manifestation of elevated homocysteine. Elevated homocysteine has been associated with vascular calcification (27). In our cohort, we observed an approximately threefold increased risk (OR 2.76, 95% CI [1.4001 to 5.4413]; $P = 0.03$) of coronary artery calcification (CAC > 1) in individuals with high homocysteine (>15 mmol/L). The same variant was detected in 3 second-degree relatives with high CAC scores (>400, 89, and 91 percentiles, respectively) found in 2 relatives, and one of them had elevated homocysteine and the other one did not complete the homocysteine test. Phenotypes of methylmalonic aciduria and homocystinuria, cblF type (MIM 277380), including failure to thrive, developmental delay, stomatitis, and skin rashes were not observed in the *LMBRD1* heterozygotes. Other unknown factors may also contribute to this family's coronary artery calcification.

Genotype and Metabolome Associations. To understand the aberrant levels of any of the 1,007 measured metabolites that are associated with physiological states of health conditions, we investigated the associations between functional genetic variants and metabolite level. We detected extreme metabolites (±6 SD) in 17.3% of individuals. A portion of the underlying mechanisms that contribute to extreme metabolites (±6 SD) is due to hormone aberrations and medication/supplement intakes. The

A

Disease Categories	Genes
Dyslipidemia	ANGPTL4, APOB (x5), APOC3 (x2), LDLR (x6), LPL (x3), MEF2A (x2), NPC1L1, PAFAH1B2, PCSK9 (x3)
Cardiomyopathy and Arrhythmia	ANK2, DSC2 (x2), ENG, GPD1L (x2), KCNE2, KCNQ1 (x2), LMNA, MYBPC3 (x9), MYH7 (x5), MYL2 (x4), MYLK (x2), PKP2, RBM20, RYR2, SCN1B, SMAD6, TCAP, TNNT2, TTN (x2), TTR (x2), VCL
Diabetes and Endocrine Diseases	ABCC8 (x2), FAAH, GLMN, HNF1A, HNF1B (x2), INSR, MC4R, NEUROD1, NOBOX, NR3C1, PCSK1 (x2), PPP1R3A (x2), PROK2, TBC1D4
Chronic Liver Diseases	HFE (3 homozygotes and 12 compound heterozygotes)
Cancer	APC, ATM (x6), BARD1, BRCA1, BRCA2 (x7), BRIP1 (x3), CHEK2 (x16), CYLD, EPCAM, FAM175A, FH (x2), GEN1, (x2), GLMN, HOXB13 (x6), LZTR1 (x4), MSH6, NBN (x4), NF1, PALB2, PMS1, PMS2, RAD50 (x2), RAD51C, RB1, RECQL, TP53
Immunological, Neurological & Other Diseases	CFHR5, COL9A1, CYP21A2 (x2), DNAH5, FCGR1A, FLG (2 homozygotes and 2 compound heterozygotes), GJB2 (2 compound heterozygotes), GRN, KIDINS220, LRP5, LRRK2 (x2), MATN3, MS4A2, MYO15A, NMNAT1 (x2), PKD1, PRPF31, RAPSN, RP1, RYR1, SCN1A, SERPINA1, SGCE, SNCA, TGM6, TNFRSF13B, WFS1
Hematological Diseases	CPOX, EGLN1, F11 (x2), G6PD (x6), HBB (x6), ITGB3, PROC (x2)
Inborn Errors of Metabolism	BTD (2 homozygotes and 3 compound heterozygotes), FMO3, DMGDH, SLC22A5

B

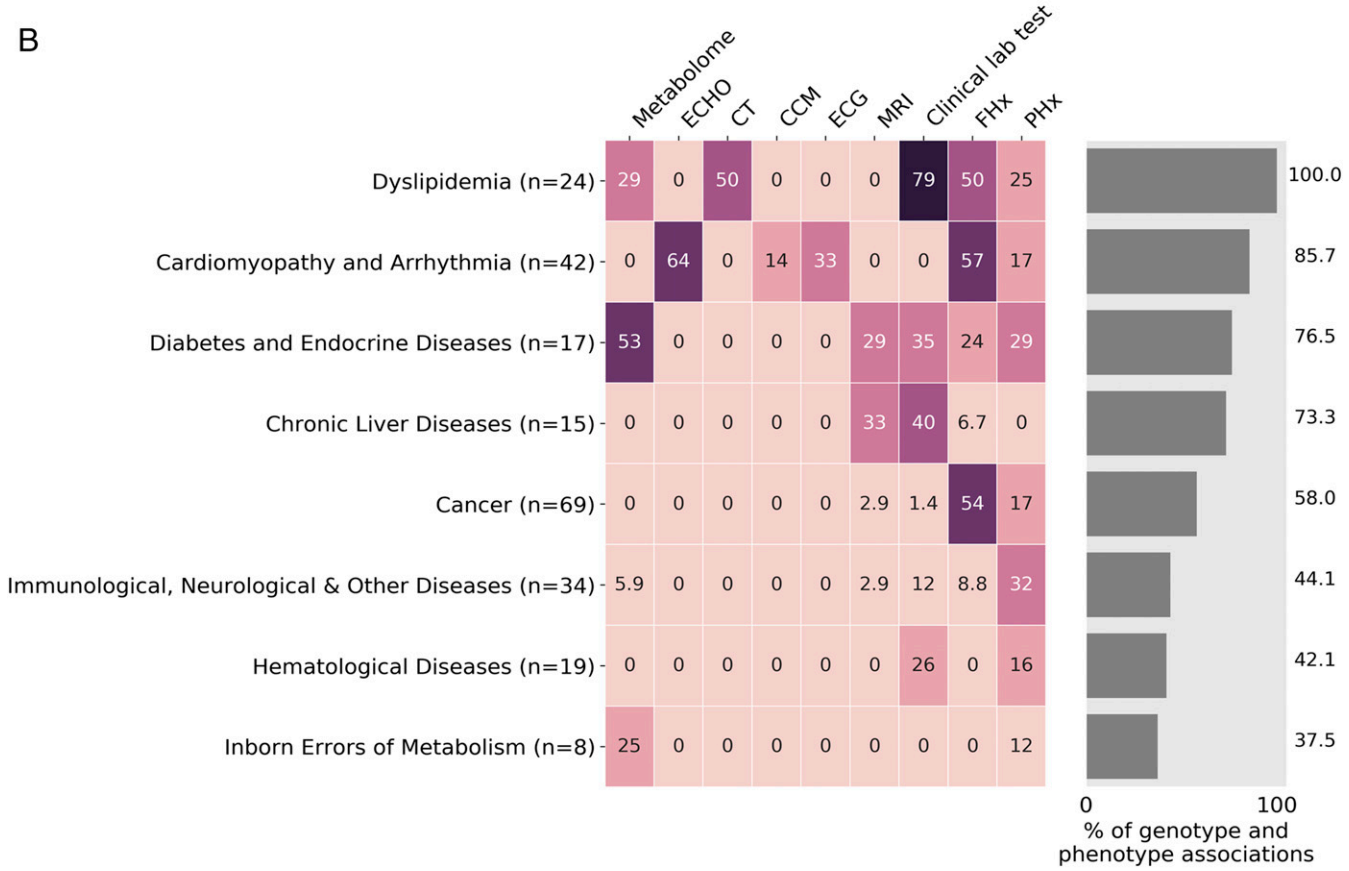

Fig. 2. Associations between medically significant genetic findings and phenotype tests by disease group and test. (*A*) Numbers of cases (gene [cases]) per disease categories are listed. (*B*) Clinical synopses in OMIM and clinical phenotypes listed in the literature are used to establish associations between MSFs and phenotype tests. The heatmap shows the fraction of cases (percentage listed) where phenotype tests detected expected clinical features for the MSF. For example, for a participant with a pathogenic variant observed in the *HNF1B* gene, the team would review his/her results in clinical laboratory tests and metabolome for profiles that are indicators of impaired glucose tolerance or impaired insulin sensitivity and an MRI test for renal cysts. Thus, he/she may have reportable findings for MRI, family history, metabolome, and clinical laboratory tests; however, the phenotype and genotype association still counts as 1 event for the bar plot. Among the 206 individuals, 21 individuals have more than 1 MSF in different disease groups. The percentages of "not tested" for the participants with MSFs are 41.7% for CT, 38.8% for metabolome, 24.2% for ECG/CCM, 12.6% for clinical laboratory test, and 0% for MRI and ECHO. FHx, family history; PHx, past and current personal medical history.

curated data of gene and metabolite relationships listed in the Kyoto Encyclopedia of Genes and Genomes (KEGG) database (28), Human Metabolome Database (HMDB) (29), and proprietary pathway database constructed by Metabolon, Inc. were used to derive candidate lists of genes whose biological functions have been implicated in the regulation of metabolites of

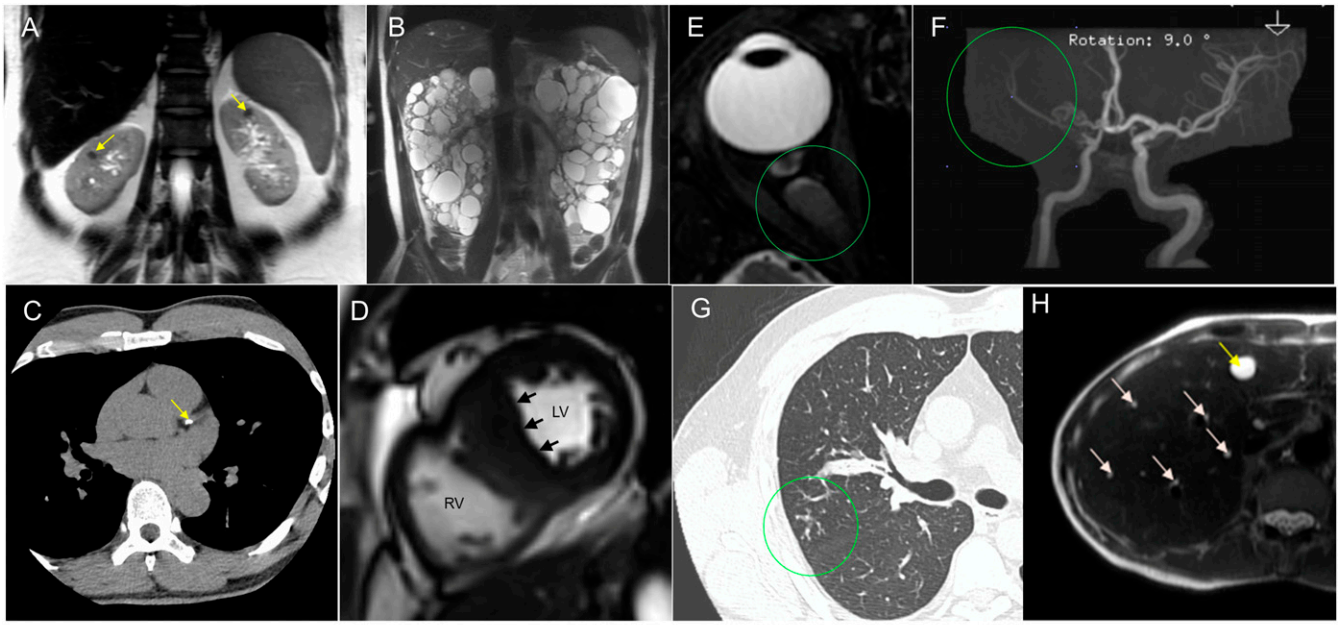

I

	Genetics			Metabolome			Blood Test	Cardiac				MRI		
	MSF	VUS-R	Carrier	Extreme Metabolite	IGT	IR		ECHO	CT	CCM	ECG	Whole Body	Brain	Cancer HN Dx
Case 1: F, age 20s Dx: None														
Case 2: F, age 50s Dx: None			*PMM2*											
Case 3: F, age 60s Dx:			*BTD LMBRD1*				5 Abnormal (cholesterol, LDL, triglyceride)		Agatson Score = 2,963			Elevated liver fat		
Case 3: F, age 30s Dx: 1. Thalassemia. 2. Renal cysts and diabetes	*HBB HNF1B*											Elevated liver fat, R2* Bilateral benign renal cysts		
Case 4: M, age 40s Dx: Polycystic kidney disease	*PKD1*				IGT = 70	IR = 72	23 Abnormal (creatinine, cystatin C , uric acid, eGFR)		Agatson Score = 488			PKD, innumerable cysts in both kidneys and the liver		
Case 5: M, age 60s Dx: Familial hypercholesterolemia	*ALDH2 PCSK9*		*BCKDHB MMAA RIN2*		IGT = 68	IR = 70	8 Abnormal (cholesterol, LDL)		Agatson Score = 111			Elevated liver R2*		
Case 6: M, age 60s Dx: Familial hypertrophic cardiomyopathy	*MYH7*		*BBS1 DNAI1 TSEN54*					Diastolic dysfunction Hypertrophic cardiomyopathy Left atrium dilation Asymmetric septal hypertrophy						
Case 7: M, age 50s Dx: Hereditary cancer-predisposing syndrome	*HFE NBN*		*CAPN3 SLX4*			IR=77	12 Abnormal					Elevated liver R2*		
Case 8: M, age 70s Dx: 1. Hemochromatosis. 2. Renal cell carcinoma	*HFE*		*C12ORF57 C2CD3 CFTR FLG VPS13B*		IGT = 91	IR = 65	15 Abnormal (Iron, iron saturation)	Aortic root dilation				Renal cell carcinoma Ascending aorta aneurysm Elevated liver R2*		Renal Cell Carcinoma
Case 9: M, age 40s Dx: Long QT	*KCNQ1*		*ALDH7A1 POMT2 SPG7*		IGT = 119		15 Abnormal				Long QT	Elevated liver fat		
Case 10: M, age 20s Dx: 1. Neurofibromatosis. 2. Vitamin E deficiency	*NF1*		*GJB2 TTPA**				12 Abnormal						Stenosis of right MCA Focal white matter lesions	
Case 11: M, age 40s Dx: 1. Thrombus 2. Hypercholesterolemia 3. Cardiomyopathy 4. Frontal lobe encephalomalacia	*APOB F5*	*TCAP*	*HFE HSPG2 C9 MEFV*		IGT= 74	IR = 64	10 Abnormal	Mild left ventricular hypertrophy	Agatson Score = 415				Frontal lobe encephalomalacia	
Case 12: M, age 60s Dx: 1. Cystic fibrosis 2. Digestive symptoms 3. Sinus infection	*CFTR*		*FANCC*				5 Abnormal					Tree-in-bud nodularity Mild bronchial wall thickening	Sinusitis	

Blue: New diagnosis from this study — Abnormal /Positive — Normal /Negative — Not Tested

Fig. 3. Examples of integrated diagnoses. (*A*) A female (40s) heterozygous for an *HNF1B* likely pathogenic variant with renal cysts and diabetes syndrome. Yellow arrows point to the bilateral renal cysts. (*B*) A male (40s) heterozygous for a likely pathogenic *PKD1* variant with polycystic kidney disease. (*C*) A male (50s) heterozygous for a pathogenic variant in the *PCSK9* gene. The yellow arrow points to the calcified left main/anterior descending coronary artery. (*D*) A male (60s) heterozygous for an *MYH7* pathogenic variant hypertrophic cardiomyopathy. (*E* and *F*) Clinical diagnosis of neurofibromatosis type 1. (*E*) Optic nerve glioma and stenosis in the right middle cerebral artery (MCA). (*F*) Decreased conspicuity of tertiary MCA branches compatible with Moyamoya syndrome. (*G*) A male (60s) compound heterozygous for *CFTR* pathogenic variants with digestive issues/bloating and chronic sinus infections. The green circle shows a tree-in-bud nodularity. (*H*) A female (60s) heterozygous for a pathogenic *PKDH1* variant with a defined liver cyst (yellow arrow) and numerous scattered subcentimeter liver cysts/hemangiomas (white arrows). (*I*) Summary of clinical findings in represented cases. Dx, diagnosis; eGFR, estimated glomerular filtration rate; F, female; LV, left ventricular; M, male; RV, right ventricular.

interest. We also took the directional effect of enzymatic reactions into consideration. Then, genomic data were investigated to identify functional genetic variants. We identified the associations between functional genetic variation and extreme metabolite levels in 31 (2.6%) individuals, mostly enriched in amino acid, lipids, and nucleotide pathways (*SI Appendix*, Table S9). *DMGDH* c.1300A>T and 1747G>T and *TTPA* c.13C>T and c.513_514insTT were classified as LP based on the ACMG

Table 2. Detection of pathogenic or likely pathogenic variants without associated disease phenotype

Disease categories	Gene and variant	Numbers of lack of phenotype cases/all observed cases
Cancer	ATM (c.3218dupT), BRCA2 (c.658_659delGT, c.4793_4794delTC), BRIP1 (c.2392C>T, c.2765T>G), CHEK2 (c.470T>C x5, c.1283C>T x2, c.1100delC), FH (c.1431_1433dupAAA x2), GLMN (c.743dupT, c.1319G>A), HOXB13 (c.251G>A x6), LZTR1 (c.238dupA, c.978_985delCAGCTCC, c.1084C>T, c.2247C>A), MSH6 (c.10C>T), RAD51C (c.571+1delG), RB1 (c.1981C>T)	29/69
Cardiomyopathy, arrhythmia, and other cardiac conditions	DSC2 (c.379G>T), GPD1L (c.839C>T), KCNE2 (c.161T>C), MYL2 (c.403-1G>C), TTN (c.55693dupA, c.73846C>T)	6/42
Diabetes and endocrine diseases	NOBOX (c.138C>A), PCSK1 (c.1063_1064dupTA), PPP1R3A (c.1985_1986delAG), PROK2 (c.163delA)	4/17
Hematological diseases	CPOX (c.661_665delCAAAT), F11 (c.901T>C x2), G6PD (c.1498C>T x4), ITGB3 (c.55delG/c.1924G>T), PROC (c.667C>T/c.761G>A)	11/19
Chronic liver diseases	HFE (c.187C>G/c.845G>A x4)	4/15
Inborn errors of metabolism	BTD (c.517G>A/c.1336G>C, c.1213T>G/c.1336G>C, c.1336G>C homo x3)	5/8
Immunological, neurological, and other diseases	DNAH5 (c.832delG/c.8440_8447delGAACCAAA), FCGR1A (c.274C>T), FLG (c.1218_1230delATCTGCAGTCAGC/c.2282_2285delCAGT, c.2282_2285delCAGT homo x2), GJB2 (c.35delG/c.101T>C, c.109G>A/c.235delC), GRN (c.1134C>A), KIDINS220 (c.757C>T), LRRK2 (c.356T>C, c.6055G>A), MYO15A (c.1137delC/c.3006delC), NMNAT1 (c.709C>T, c.716T>C), PRPF31 (c.600_612delCAAGCACCGCATC), RYR1 (c.14126C>T), SERPINA1 (c.863A>T/c.1096G>A), SGCE (c.21G>A), SNCA (c.150T>G)	19/34

homo, homozygotes.

guidelines. The rest of the variants listed in *SI Appendix*, Table S9 were classified as VUS. We also evaluated the phenotypic manifestation for individuals who carried P/LP variants associated with metabolic disorders using metabolic feature and laboratory abnormalities listed in the OMIM synopsis (24). This approach established associations in 34 (2.9%) individuals with elevated/decreased metabolites (95% CI) (*SI Appendix*, Table S10) enriched in amino acid, cofactor and vitamin, and lipid pathways. The genetic basis of some metabolite variation was identified. An interesting case illustrating the value of this approach was the demonstration of an association of an LoF nonsense variant, c.13C>T (p.Arg5*), in the *TTPA* gene associated with ataxia with isolated vitamin E deficiency (MIM 277460). Three family members had the maternally segregated variant, and all had markedly reduced levels of vitamin E ranging from −3.6 to −6 SD. Clinical ataxia was not observed in these participants.

Genes Associated with Metabolites and the Ratio of Cholesterol and Hydroxy-3-Methylglutarate. The collection of deep phenotype data allowed us to pursue additional research avenues. To expand our sample set for these analyses, we also included metabolome data from 1,969 European ancestry twins enrolled in the TwinsUK Registry, a British national register of adult twins (30). We used a gene-based collapsing analysis to identify genes where rare functional variants were associated with a statistically significant difference in the levels of any of the 1,007 measured metabolites. We identified significant associations between the phenylketonuria gene *PAH* and the metabolites phenylalanine and gamma-glutamylphenylalanine as well as between the glutaric acidemia gene *ETFDH* and octanoylcarnitine, decanoylcarnitine, and nonanoylcarnitine (Fig. 4). We identified 19 significant associations with 11 other genes (*SI Appendix*, Table S11). The identified associations largely reflected known conditions, such as dimethylglycine dehydrogenase deficiency and histidinemia. However, 5 associations were identified: between the 1,5-anhydroglucitol and *SLC5A10*; between the amino acids alpha-hydroxyisovalerate and 2-hydroxy-3-methylvalerate and *HAO2*; between the amino acid 5-hydroxylysine and *HYKK*; between *N*-acetyl-beta-alanine and *PTER*; and between alpha-ketoglutaramate and *NIT2*. NIT2 is known to break down alpha-ketoglutaramate, and we have identified LoF variants.

To measure the efficacy of hydroxy-3-methylglutaryl coenzyme A (HMG-CoA) reductase inhibitors such as statins, we measured the precursor, hydroxy-3-methylglutarate (HMG), and the product, cholesterol. We calculated the ratios of cholesterol and HMG (CHO:HMG) as an indicator for HMG-CoA reductase inhibitor efficacy. Statins have been used to reduce low-density lipoproteins (LDLs), one of the major risk factors for coronary heart disease (31). Individuals on statin therapy ($n = 52$) and on ezetimibe therapy ($n = 9$) had a lower CHO:HMG ratio (t test, mean 0.85, $P = 0.001$ and mean 0.80, $P = 0.02$, respectively)

Table 3. Autosomal recessive conditions with phenotype manifestation for imaging and clinical lab tests

	Sex	Age, y	Variant	Phenotype correlation
PKDH1_1	F	50s	c.7_19delGCCTGGCTGATCT (p.Ala3fs)	1-cm benign hepatic hemangioma in the right lobe; innumerable tiny cystic lesions in the liver
PKDH1_2	M	40s	c.7_19delGCCTGGCTGATCT (p.Ala3fs)	Innumerable hepatic cysts; 1-cm benign renal cyst in the right kidney
PKDH1_3	F	40s	c.107C>T (p.Thr36Met)	Several benign hepatic cysts
PKDH1_4	F	60s	c.6992T>A (p.Ile2331Lys)	Scattered benign renal cysts; innumerable benign hepatic cysts
PKDH1_5	M	70s	c.3766delC (p.Gln1256fs)	Several benign cysts in the left kidney
PKDH1_6	M	30s	c.4870C>T (p.Arg1624Trp)	No abnormal findings
PKDH1_7	M	50s	c.4870C>T (p.Arg1624Trp)	No abnormal findings
PKDH1_8	F	20s	c.6992T>A (p.Ile2331Lys)	No abnormal findings
PKDH1_9	F	30s	c.6992T>A (p.Ile2331Lys)	No abnormal findings
PKDH1_10	M	20s	c.8518C>T (p.Arg2840Cys)	Multiple biliary hamartomas in the liver
PKDH1_11	M	50s	c.8870T>C (p.Ile2957Thr)	Two benign renal cysts
PKDH1_12	F	70s	c.9530T>C (p.Ile3177Thr)	Innumerable cysts in the liver
PKDH1_13	F	20s	c.11665+1G>A	No abnormal findings
ALPL_1	M	50s	c.571G>A (p.Glu191Lys)	Alkaline phosphatase 36 IU/L
ALPL_2	F	60s	c.571G>A (p.Glu191Lys)	NA
ALPL_3	M	50s	c.571G>A (p.Glu191Lys)	Alkaline phosphatase 35 IU/L
ALPL_4	F	50s	c.984_986delCTT (p.Phe328del)	Alkaline phosphatase 18 IU/L
LMBRD1_1	M	70s	c.63dupA (p.Leu22fs)	CAC 413; homocysteine 16.1 μmol/L
LMBRD1_2	M	60s	c.63dupA (p.Leu22fs)	CAC 683; homocysteine 10.7 μmol/L
LMBRD1_3	F	30s	c.63dupA (p.Leu22fs)	CAC NA; homocysteine 7.1 μmol/L
LMBRD1_4	F	60s	c.63dupA (p.Leu22fs)	CAC 2,963; homocysteine 16.5 μmol/L

Alkaline phosphatase (normal range 39 to 117 IU/L); homocysteine (normal range 0 to 15 μmol/L); CAC, coronary artery calcium; NA, not available.

compared with 603 individuals without any cholesterol-lowing therapy (mean 1.17) (*SI Appendix*, Fig. S3*A*) (31–33). Two individuals treated with the PCSK9 monoclonal inhibitor had low CHO:HMG ratios in in 1st and 5th percentiles, respectively. Two untreated participants with *LDLR* P/LP variants had high CHO:HMG ratios in 94th and 96th percentiles, respectively (*SI Appendix*, Fig. S3*B*). To expand our analysis, we included metabolome data from the TwinsUK Registry; we observed that HMG is associated with longitudinal cardiovascular events ($P = 0.01$) after controlling for baseline body mass index (BMI), sex, and age. To identify associations between genes and CHO:HMG ratios, we also used a gene-based collapsing analysis. The genome-wide analysis identified 18 genes ($P < 0.01$ with at least 5 independent carriers) associated with high CHO:HMG ratio, and 9 genes associated with low CHO:HMG ratio (*SI Appendix*, Table S12).

Discussion

Our results show that when we followed the ACMG guideline to assess the probability of pathogenicity surveying genome-wide for disease-causing genes and variants, ∼1 in 6 adult individuals (206 [17.3%]) had at least 1 genetic variant with pathogenicity. When we integrated genetic analysis with deep phenotyping using metabolomics and advanced imaging in addition to past medical and family history, 137 (11.5%) participants had genotype and phenotype associations supporting clinicians' ability to make a diagnosis of genetic disorders in our adult self-referred cohort. The percentage of genotype and phenotype associations ranged from 37.5 to 100% depending on disease categories. Among disease categories, dyslipidemia, cardiomyopathy and arrhythmia, and diabetes and endocrine diseases had percentages of associations higher than 75%. Moreover, we demonstrate that advanced imaging plays an important role in the detection of early-stage physiological measurements such as atherosclerotic disease and cardiomyopathy of adult genetic disorders, providing evidence to physicians for the differential diagnosis of genetic disorders when integrating genomic findings with deep phenotyping. Compared with large-scale gene panel approaches using EHRs such as the DiscovEHR (12) and UK Biobank studies (13), our genome-wide analysis combined with the prospective deep phenotype assessment had increased sensitivity (10.9 vs. 2.3%, respectively, approximately fivefold) to identify previously undiagnosed adults with genetic disorders.

The genome-wide approach also resulted in identification of variants which might confer a burden based on possible ambiguous results because of the lack of genotype and phenotype associations. Genetic testing that identifies a P/LP variant is not equivalent to diagnosing the patient with the associated genetic disorder. Physicians need to properly integrate that predictive power of genetic findings with the patient medical data for differential diagnosis (34). In our cohort, 69 (5.8%) individuals had P/LP variants but did not have associated family history, medical history, or phenotypes detected in tests. There are 3 possible explanations for the lack of disease symptoms in this population. First, the probability of nonpathogenicity (1 to 10% for a likely pathogenic variant) (34, 35), reduced penetrance, variable expressivity, or late onset of disease presentation may be reasons for the lack of genotype and phenotype associations. For example, the c.470T>C and c.1283C>T variants in the *CHEK2* gene have been reported to cause an increased risk of cancer from large meta-analyses but to be associated with a much lower risk (reduced penetrance) than other *CHEK2* pathogenic variants (36). Second, family and medical history intake may not be comprehensive enough to be used to establish the clinical diagnosis of a genetic disease. Additional personal and family history for potential phenotype associations with the variant may need to be obtained for further assessments. None of the 6 individuals with the *HOXB13* c.251G>A variant reported family or medical history of prostate cancer. Cardiovascular diseases, hypertension, and diabetes were the most frequent family history documentation in the health system (37). From our data, the fraction of genotype and phenotype associations from family history ranged from 24 to 57% in dyslipidemia, cardiomyopathy and arrhythmia, diabetes, and endocrine diseases, and our deep phenotype tests detected clinical and preclinical presentations,

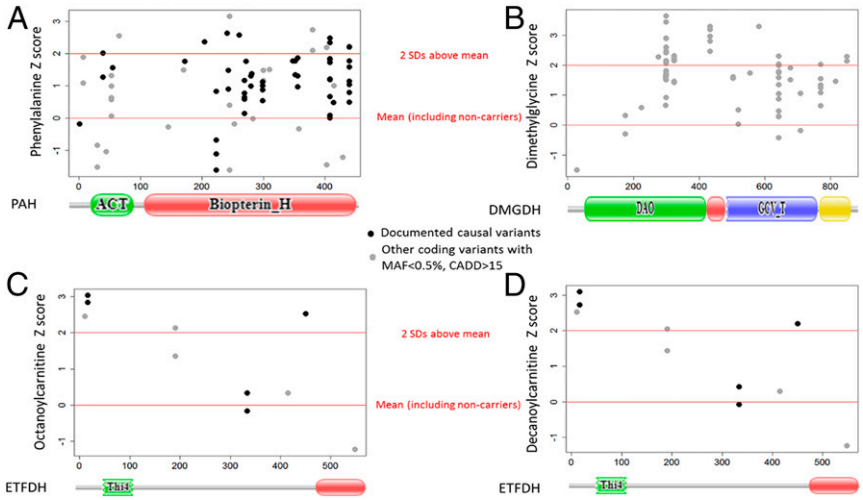

Fig. 4. Metabolite levels in heterozygous carriers of rare coding variants in recessive inborn errors of metabolism genes. Shown is the normalized *Z* score of the metabolite levels of each individual who carries a coding variant in each gene (*y* axis), with the amino acid position shown on the *x* axis. All variants have minor allele frequency (MAF) <0.5%, and all have Combined Annotation Dependent Depletion (CADD) scores >15. Red lines indicate cutoffs for normalized *Z* scores above 0, indicating increased levels of phenylalanine relative to the mean, and 2, indicating outliers of interest. Known causal variants are shown in black according to http://www.biopku.org/home/home.asp for *PAH* and ClinVar or HGMD for *ETFDH* and *DMGDH* (none of the *DMGDH* variants shown here were found in ClinVar or HGMD). Gene annotations were generated from pfam.xfam.org. (*A*) Phenylalanine levels of *PAH* variant carriers. Green, ACT domain; red, biopterin-dependent aromatic amino acid hydroxylase. (*B*) Dimethylglycine levels of *DMGDH* variant carriers. Green, FAD-dependent oxidoreductase; red, Flavin adenine dinucleotide (FAD)-dependent oxidoreductase central domain; blue, aminomethyltransferase folate-binding domain; yellow, glycine cleavage T-protein C-terminal barrel domain. (*C* and *D*) Octanoylcarnitine (*C*) and decanoylcarnitine (*D*) levels of *ETFDH* variant carriers. Green, Thi4 family; red, electron transfer flavoprotein-ubiquinone oxidoreductase, 4Fe-4S.

further enhancing the clinical diagnosis of genetic disorders in adults (Fig. 2*B*). Third, protective (i.e., resilience) alleles may exist in the genomes of these asymptomatic individuals and are yet to be discovered.

With deep phenotyping, we found that heterozygous carriers of autosomal recessive diseases exhibited detectable phenotypic changes. Heterozygous carriers of autosomal recessive conditions are usually healthy with no related symptoms of the disease. Some carriers may have subtle or milder symptoms of the disease. We identified 8 *PKDH1* (average age 53.1 y) heterozygotes with hepatic and/or renal cysts from the WB-MRI results. The remaining 5 *PKDH1* carriers (average age 35.6 y) had no detectable cysts at the time of evaluation. From the genomics and metabolomics associations, we identified 61 (5.1%) heterozygotes with metabolite manifestations affecting serum metabolite levels. In particular, 10 out of 30 (33%) *PAH* carriers had elevated phenylalanine detected by metabolomics, similar to observations using the phenylalanine tolerance test (38), further confirming the pathogenicity of the genetic variants. Our data have not been explored extensively to evaluate if a long-term phenotype manifestation in heterozygous carriers of autosomal recessive conditions may cause an impact on health. For example, heterozygous carriers of *HFE* C282Y have been shown to have mild phenotypes of iron overload, resulting in an increased risk of hepatocellular carcinoma (39). Longitudinal evaluation of these individuals will be required to characterize the clinical significance of undefined findings.

A fraction of the reportable metabolomic results was associated with glucose and insulin dysregulation. These personalized measurements may enable individuals to optimize diet and lifestyle adjustment on the basis of personalized glycemic response. For example, the personalized measurement using metabolomics facilitated the clinical diagnosis of maturity-onset diabetes of the young, where a precision diagnosis can provide appropriate treatment such as low-dose sulfonylurea without the possibility of incorrect treatment using insulin. As for cholesterol homeostasis, we found that measurement of the CHO:HMG ratio tracked with the changes observed with use of cholesterol-lowering medications. Our study also identified several candidate genes associated with the CHO:HMG ratio, suggesting possible mechanistic pathways that regulate cholesterol homeostasis. Further, HMG was associated with cardiovascular events using the TwinsUK Registry. Further studies are required to determine if HMG or the CHO:HMG ratio is a useful biomarker for measuring the efficiency of cholesterol control and management. Other examples are the inhibitors of xanthine oxidase, such as allopurinol, commonly used in the treatment of diseases associated with high levels of uric acid (i.e., urate), including gout and tumor lysis syndrome. Metabolite levels of xanthine, hypoxanthine, orotidine, orotic acid (i.e., orotate), and urate may be useful to monitor drug efficacy (*SI Appendix*, Fig. S3*C*).

Medicine is traditionally practiced on individuals who are already symptomatic. Clinicians integrate silo test results for differential diagnosis and devise treatments accordingly. Our approach of integration of omics and advance imaging achieved some notable near-term successes on the identification and clinical assessment of adults with previously undiagnosed genetic disorders. Furthermore, our data also provided plausible genetic causes for abnormal physiological measurements at the individual level of analysis. Our study did not measure health outcomes, benefits, and cost-effectiveness. Repeat evaluation of these individuals is required to characterize the clinical significance of the findings. Overall, our study may be evaluated in the context of methodological considerations for precision medicine initiatives and have the potential to change clinical assessments beyond genome sequencing.

Materials and Methods

Study Population and Process. We enrolled self-referred adults ≥18 y old without acute illness, activity-limiting unexplained illness or symptoms, or known active cancer between September 2015 and March 2018. Participants underwent a verbal review of the institutional review board (IRB)-approved consent. During the consent process, we explained to individuals with known genetic disorders that our test is not suitable for clinical testing and referred them to facilities with clinical genetic tests. The study protocol was

approved by the Western IRB (WIRB), and all subjects gave informed consent. We received permission from the WIRB to collect up to $25,000 for participation with an average of $8,000 for participation in this study. Past medical and family history (the 3-generation pedigree), risk factors, medical symptoms, and medication list were collected prior to or during the visit. Data on medical history of participants in this study included self-reported, medical charts from participants' physicians, or electronic health records. Noninvasive quantitative whole-body and brain MRI/magnetic resonance angiography, CT coronary artery calcium scoring, electrocardiogram, echocardiogram, and clinical laboratory tests were employed as phenotype tests. Phenotype tests were performed as described in Perkins et al. (19), our pilot study. For clinical laboratory tests, participants performed approximately 120 tests that covered liver, kidney, hematology, endocrine, immunology, lipid, and metal functions. Additional materials and methods have been placed in *SI Appendix*.

Data Availability. Detailed information of the reporting findings and medically significant variants is provided in *SI Appendix*.

ACKNOWLEDGMENTS. We acknowledge the individuals who participated in this precision medicine study, without whom the findings would not be possible. Julie Ellison provided medical editing assistance. We acknowledge Human Longevity and Health Nucleus staff past and present: Alexander Graff, Amy Reed, Ana Sanchez, Athena Hutchinson, Carina Sarabia, Catherine Vrona, Cheryl Buffington, Cheryl Greenberg, Christina Bonas, Daniel Jones, Danielle Dorris, Desiree Cheney, Diana Cardin Escobedo, Dmitry Tkach, Eric Dec, Genelle Olsen, Greg Olson, Heidi Millard, Helen Messier, Hyun-Kyung Chung, Jason Deckman, Javier Velazquez-Muriel, Jian Wu, Kathy Levine, Keisha Robinson, Krista-Lynn Banner, Kristi Ericksen-Miller, Laura Edwards, Melissa Schweitzer, Nicole Boramanand, Nolan Tengonciang, Patrick Jamieson, Samantha Punsalan, Tom Folan, Victor Lavrenko, Wayne Delport, and William Herrera.

1. J. C. Venter, H. O. Smith, M. D. Adams, The sequence of the human genome. *Clin. Chem.* **61**, 1207–1208 (2015).
2. International Human Genome Sequencing Consortium, Finishing the euchromatic sequence of the human genome. *Nature* **431**, 931–945 (2004).
3. J. E. Posey *et al*., Molecular diagnostic experience of whole-exome sequencing in adult patients. *Genet. Med.* **18**, 678–685 (2016).
4. S. B. Seidelmann *et al*., Application of whole exome sequencing in the clinical diagnosis and management of inherited cardiovascular diseases in adults. *Circ. Cardiovasc. Genet.* **10**, e001573 (2017).
5. T. M. Bardakjian *et al*., Genetic test utilization and diagnostic yield in adult patients with neurological disorders. *Neurogenetics* **19**, 105–110 (2018).
6. E. S. Zoltick *et al*.; PeopleSeq Consortium, Predispositional genome sequencing in healthy adults: Design, participant characteristics, and early outcomes of the PeopleSeq Consortium. *Genome Med.* **11**, 10 (2019).
7. M. P. Ball *et al*., A public resource facilitating clinical use of genomes. *Proc. Natl. Acad. Sci. U.S.A.* **109**, 11920–11927 (2012).
8. A. L. Cirino *et al*.; MedSeq Project*, A comparison of whole genome sequencing to multigene panel testing in hypertrophic cardiomyopathy patients. *Circ. Cardiovasc. Genet.* **10**, e001768 (2017).
9. J. J. Johnston *et al*., Individualized iterative phenotyping for genome-wide analysis of loss-of-function mutations. *Am. J. Hum. Genet.* **96**, 913–925 (2015).
10. S. Rego *et al*., High-frequency actionable pathogenic exome variants in an average-risk cohort. *Cold Spring Harb. Mol. Case Stud.* **4**, a003178 (2018).
11. J. L. Vassy *et al*.; MedSeq Project, The impact of whole-genome sequencing on the primary care and outcomes of healthy adult patients: A pilot randomized trial. *Ann. Intern. Med.* **167**, 159–169 (2017).
12. F. E. Dewey *et al*., Distribution and clinical impact of functional variants in 50,726 whole-exome sequences from the DiscovEHR study. *Science* **354**, aaf6814 (2016).
13. C. V. Van Hout, *et al*., Whole exome sequencing and characterization of coding variation in 49,960 individuals in the UK Biobank. bioRxiv:10.1101/572347 (23 May 2019).
14. N. D. Price *et al*., A wellness study of 108 individuals using personal, dense, dynamic data clouds. *Nat. Biotechnol.* **35**, 747–756 (2017).
15. C. Manzoni *et al*., Genome, transcriptome and proteome: The rise of omics data and their integration in biomedical sciences. *Brief. Bioinform.* **19**, 286–302 (2018).
16. C. Betzen *et al*., Clinical proteomics: Promises, challenges and limitations of affinity arrays. *Proteomics Clin. Appl.* **9**, 342–347 (2015).
17. R. A. Kellogg, J. Dunn, M. P. Snyder, Personal omics for precision health. *Circ. Res.* **122**, 1169–1171 (2018).
18. T. Long *et al*., Whole-genome sequencing identifies common-to-rare variants associated with human blood metabolites. *Nat. Genet.* **49**, 568–578 (2017).
19. B. A. Perkins *et al*., Precision medicine screening using whole-genome sequencing and advanced imaging to identify disease risk in adults. *Proc. Natl. Acad. Sci. U.S.A.* **115**, 3686–3691 (2018).
20. L. Guo *et al*., Plasma metabolomic profiles enhance precision medicine for volunteers of normal health. *Proc. Natl. Acad. Sci. U.S.A.* **112**, E4901–E4910 (2015).
21. O. Gottesman *et al*.; eMERGE Network, The Electronic Medical Records and Genomics (eMERGE) Network: Past, present, and future. *Genet. Med.* **15**, 761–771 (2013).
22. UK10K Consortium, The UK10K project identifies rare variants in health and disease. *Nature* **526**, 82–90 (2015).
23. P. Greenland *et al*.; American College of Cardiology Foundation Clinical Expert Consensus Task Force (ACCF/AHA Writing Committee to Update the 2000 Expert Consensus Document on Electron Beam Computed Tomography); Society of Atherosclerosis Imaging and Prevention; Society of Cardiovascular Computed Tomography, ACCF/AHA 2007 clinical expert consensus document on coronary artery calcium scoring by computed tomography in global cardiovascular risk assessment and in evaluation of patients with chest pain: A report of the American College of Cardiology Foundation Clinical Expert Consensus Task Force (ACCF/AHA Writing Committee to Update the 2000 Expert Consensus Document on Electron Beam Computed Tomography) developed in collaboration with the Society of Atherosclerosis Imaging and Prevention and the Society of Cardiovascular Computed Tomography. *J. Am. Coll. Cardiol.* **49**, 378–402 (2007).
24. A. Hamosh, A. F. Scott, J. S. Amberger, C. A. Bocchini, V. A. McKusick, Online Mendelian Inheritance in Man (OMIM), a knowledgebase of human genes and genetic disorders. *Nucleic Acids Res.* **33**, D514–D517 (2005).
25. P. Greenland *et al*.; American College of Cardiology Foundation/American Heart Association Task Force on Practice Guidelines, 2010 ACCF/AHA guideline for assessment of cardiovascular risk in asymptomatic adults: Executive summary: A report of the American College of Cardiology Foundation/American Heart Association Task Force on Practice Guidelines. *Circulation* **122**, 2748–2764 (2010).
26. H. Hecht *et al*., Clinical indications for coronary artery calcium scoring in asymptomatic patients: Expert consensus statement from the Society of Cardiovascular Computed Tomography. *J. Cardiovasc. Comput. Tomogr.* **11**, 157–168 (2017).
27. S. Guthikonda, W. G. Haynes, Homocysteine: Role and implications in atherosclerosis. *Curr. Atheroscler. Rep.* **8**, 100–106 (2006).
28. M. Kanehisa, Y. Sato, M. Kawashima, M. Furumichi, M. Tanabe, KEGG as a reference resource for gene and protein annotation. *Nucleic Acids Res.* **44**, D457–D462 (2016).
29. D. S. Wishart *et al*., HMDB 4.0: The Human Metabolome Database for 2018. *Nucleic Acids Res.* **46**, D608–D617 (2018).
30. A. Moayyeri, C. J. Hammond, A. M. Valdes, T. D. Spector, Cohort profile: TwinsUK and Healthy Ageing Twin Study. *Int. J. Epidemiol.* **42**, 76–85 (2013).
31. J. A. Friesen, V. W. Rodwell, The 3-hydroxy-3-methylglutaryl coenzyme-A (HMG-CoA) reductases. *Genome Biol.* **5**, 248 (2004).
32. L. J. Engelking, M. R. McFarlane, C. K. Li, G. Liang, Blockade of cholesterol absorption by ezetimibe reveals a complex homeostatic network in enterocytes. *J. Lipid Res.* **53**, 1359–1368 (2012).
33. J.-P. Drouin-Chartier *et al*., Ezetimibe increases intestinal expression of the LDL receptor gene in dyslipidaemic men with insulin resistance. *Diabetes Obes. Metab.* **18**, 1226–1235 (2016).
34. L. G. Biesecker, R. L. Nussbaum, H. L. Rehm, Distinguishing variant pathogenicity from genetic diagnosis: How to know whether a variant causes a condition. *J. Am. Med. Assoc.* **320**, 1929–1930 (2018).
35. S. Richards *et al*.; ACMG Laboratory Quality Assurance Committee, Standards and guidelines for the interpretation of sequence variants: A joint consensus recommendation of the American College of Medical Genetics and Genomics and the Association for Molecular Pathology. *Genet. Med.* **17**, 405–424 (2015).
36. J. Balmaña *et al*., Conflicting interpretation of genetic variants and cancer risk by commercial laboratories as assessed by the Prospective Registry of Multiplex Testing. *J. Clin. Oncol.* **34**, 4071–4078 (2016).
37. R. Endevelt, I. Goren, T. Sela, V. Shalev, Family history intake: A challenge to personalized approaches in health promotion and disease prevention. *Isr. J. Health Policy Res.* **4**, 60 (2015).
38. H. Berry, B. Sutherland, G. M. Guest, Phenylalanine tolerance tests on relatives of phenylketonuric children. *Am. J. Hum. Genet.* **9**, 310–316 (1957).
39. C. Hellerbrand, A. Pöppl, A. Hartmann, J. Schölmerich, G. Lock, HFE C282Y heterozygosity in hepatocellular carcinoma: Evidence for an increased prevalence. *Clin. Gastroenterol. Hepatol.* **1**, 279–284 (2003).